processes

MDPI

Article

Temperature Field Calculation and Thermal Circuit Equivalent Analysis of 110 kV Core Cable Joint

Zhiqiang Zhang [1], Xiaolong Deng [1], Lili Liang [1], Xuezong Wang [2,3], Yu Chen [1] and Jiangjun Ruan [3,*]

[1] Guangdong Zhongshan Power Supply Bureau of China Southern Power Grid Co., Ltd., Zhongshan 528401, China; alex_ccu@163.com (Z.Z.)
[2] China Electric Power Research Institute, Wuhan 430074, China
[3] School of Electrical Engineering and Automation, Wuhan University, Wuhan 430072, China
* Correspondence: ruan308@126.com

Abstract: In order to indirectly calculate the core temperature of a cable joint, an equivalent transient thermal circuit model of single-core cable joint by considering axial heat dissipation is proposed. Firstly, the temperature field of the middle joint of a 110 kV single-core cable is calculated by finite element method. Based on the heat dissipation path of the core, an improved equivalent thermal circuit model is proposed. The axial heat dissipation of the cable joint core is simplified to a thermal resistance and the temperature rise of the cable body core, the temperature calculation of the cable joint transient process is realized. Compared with the results of finite element simulation, the steady-state temperature errors of the thermal circuit model are within 1 °C, while the maximum temperature errors of the transient process shall not exceed 3 °C, which proves the validity of the model. This method can provide reference for temperature inversion and the dynamic current-carrying capacity prediction of cable joints.

Keywords: single-core cable joint; finite element simulation; axial heat transfer; thermal circuit model; transient temperature rise

check for updates

Citation: Zhang, Z.; Deng, X.; Liang, L.; Wang, X.; Chen, Y.; Ruan, J. Temperature Field Calculation and Thermal Circuit Equivalent Analysis of 110 kV Core Cable Joint. *Processes* **2024**, *12*, 463. https://doi.org/10.3390/pr12030463

Academic Editor: Wen-Jer Chang

Received: 23 January 2024
Revised: 17 February 2024
Accepted: 21 February 2024
Published: 24 February 2024

Copyright: © 2024 by the authors. Licensee MDPI, Basel, Switzerland. This article is an open access article distributed under the terms and conditions of the Creative Commons Attribution (CC BY) license (https://creativecommons.org/licenses/by/4.0/).

1. Introduction

As the "blood vessels" and "meridians" of the power grid, the operation and health status of power cables are directly related to the safe and stable operation of the distribution network [1,2]. Cable joints are the weakest link in the insulation of cable systems, and their faults have always been high in the proportion of cable faults [3–5]. The core temperature is a key feature of cable joint status monitoring. An increase in temperature may accelerate insulation aging at the joint and increase the failure rate. It is the main factor that restricts the current-carrying capacity of cables [6–9].

Based on the structure of cable joints and the thermal resistance and loss models of each layer material, an equivalent thermal circuit model can be established to calculate the core temperature. Currently, the widely used method is to simplify the steady-state/transient thermal circuit model based on the IEC-60287 [10] or IEC-60853 [11,12] standards. By conducting experiments or finite element simulations, the parameters in the thermal circuit model can be calculated to achieve core temperature calculation and current-carrying capacity prediction [13–15]. However, current thermal path models are only one-dimensional models that consider radial heat dissipation. For axial heat dissipation, due to the small thermal resistance of the conductor, it is often assumed that the temperature difference between the conductors near the joint is very small, thus approximating the axial temperature of the joint as equal and ignoring axial heat dissipation [16]. Reference [17] used the thermal path method to analyze and compare the radial thermal resistance differences between the cable joint and the connected cable body. And the influence of axial heat transfer on the local temperature distribution of the joint was analyzed. Reference [18] takes a T-shaped cable joint as the research object; the influence of material parameter changes in each layer

on the temperature field calculation results during transient processes was analyzed, and the improved thermal circuit model was proposed. In reference [19], a 3D thermal model of underground power cable is presented. The structure of each layer of cable joint is simulated as several elementary cylindrical volumes. Based on the elementary cylindrical volume, a thermal path model considering radial and axial heat dissipation is established in the paper, and analytical formulas for radial and axial thermal resistance are provided. References [20,21] analyzed the axial heat transfer of cable joints through finite element simulation and steady-state temperature rise tests, respectively, and found that axial heat dissipation also affects the core temperature. Considering the axial heat transfer of the wire core effectively improves the calculation accuracy of the wire core temperature, thereby achieving a more accurate prediction of the current-carrying capacity [22]. Although the finite element method can accurately calculate the temperature distribution of a cable joint, the calculation speed and accuracy of this method are affected by the number of finite element model elements, making it difficult to achieve real-time and accurate calculations in engineering, which affects the application of this method. In practical engineering, the main focus is often on the highest temperature at the crimping point of cable joints and the surface temperature of each layer structure. Therefore, the calculation efficiency can be greatly improved by establishing a thermal path model instead of real-time finite element calculations. However, further research is needed to establish a thermal path model for cable joints that considers axial heat dissipation.

In summary, this paper proposes a transient thermal path model for cable joints that considers axial heat dissipation, in response to the problem that existing cable joint thermal path models only consider radial heat dissipation. Taking 110 kV single-core cables as the research object, the heat dissipation path of the wire core is determined through finite element temperature field calculation, and a simplified thermal circuit model is proposed to calculate the transient temperature changes on the surface of each layer structure in the joint. Compared to finite element methods, thermal path models can effectively improve computational efficiency. The research results can provide reference for predicting the current-carrying capacity of cables.

2. Analysis of Heat Dissipation Path for 110 kV Single-Core Cable Joints

2.1. Temperature Field Calculation of Cable Joints

Firstly, temperature field calculation based on the finite element method is carried out for the main body and intermediate joints of 110 kV single-core cables to obtain the core temperature [23,24]. The cable model for the calculation model is YJLW03-Z 64/110 kV 630 mm^2. Structurally speaking, the cable joint and body are a two-dimensional axisymmetric temperature field [25,26]. The schematic diagram of the geometric structure is shown in Figure 1, and the relevant parameters of each material are shown in Table 1. When calculating, the cable is exposed to air, so a third type of boundary condition [27] is applied to the outer surface of the body and joint, which is an ambient temperature of 25 °C and a convective heat transfer coefficient of 10 $W/(m^2 \cdot °C)$.

Table 1. Material parameters of cable and joint.

Structure	Thermal Conductivity W/(m·K)	Density kg/m^3	Specific Heat Capacity J/(kg·K)
Wire core (copper)	383	8889	390
XLPE	0.4	920	2500
Water blocking tape	0.6	600	2000
Aluminum sheath	218	2780	883
Outer sheath	0.5	950	1842

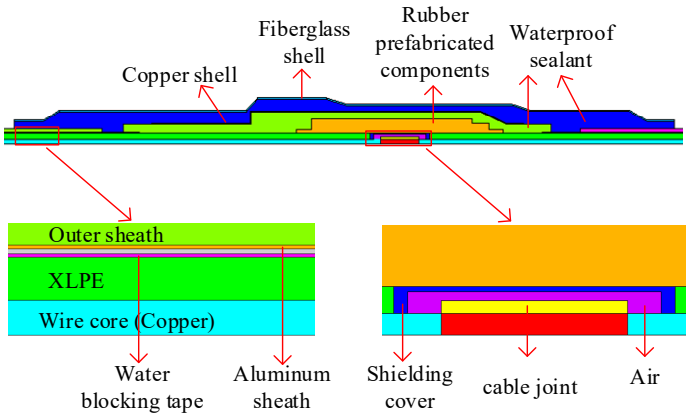


Figure 1. Structure of 110 kV cable joint.

The heat sources generated during cable operation mainly include the core heat source of the cable, the medium loss heat source of each layer of medium, and the sheath circulating heat source of the grounding layer [28]. Due to the high current conditions during cable operation, the heat source mainly comes from the wire core, so the influence of medium loss and circulating current is ignored. The heat source generated by the wire core can be divided into two types: the heat source generated by the conductor passing through the wire core and the heat source generated by the contact resistance passing through the cable joint pressure connection. The schematic diagram of the heat source loading is shown in Figure 2. The heat generation rates corresponding to the two types of heat sources are as follows.

$$G_1 = \frac{P_1}{V_1} = \frac{I^2 R_1}{\pi {r_1}^2} = \frac{I^2}{\pi {r_1}^2} \times \frac{\rho}{\pi {r_1}^2} = \frac{I^2 \rho}{\pi^2 {r_1}^4} \tag{1}$$

$$G_2 = \frac{P_2}{V_2} = \frac{I^2 R_j}{\pi {r_2}^2 l} \tag{2}$$

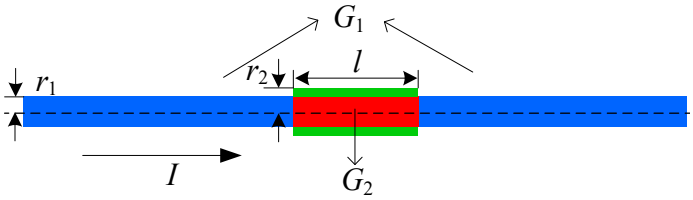


Figure 2. Schematic diagram of heat source in cable.

Among them, P_1 and P_2 are the heating powers of the contact resistance of the wire core conductor and the pressure connecting pipe, respectively; V_1 and V_2 are the volumes corresponding to the two types of heat sources; I is the current effective value through the cable; ρ is the electrical resistivity of copper conductors; l is the total length of the pressure connecting pipe; r_1 and r_2 correspond to the radii of the cable core and pressure connecting pipe, respectively; and R_j is the total resistance at the pressure connection point. The calculation yields $G_1 = 0.035\ I^2$ and $G_2 = 0.0217\ I^2$.

According to the structure of 110 kV cable joint in Figure 1, the finite element method of 110 kV cable joint is built. In order to accurately consider the axial heat dissipation of cables and control the computational workload of the model, the cable length in the finite element model is taken as 10 m, so that the axial heat dissipation at the end is reduced to near 0. Then, at a single step current of 1000 A, transient temperature field calculation is carried out for a total duration of 150 h. The time step in the model is taken as 600 s. The temperature–time variation curves at different positions of the wire core are calculated and shown in Figure 3. It can be seen that after 150 h, the core temperature basically reaches a steady state, and the temperature field distribution at the joint is shown in Figure 4. The temperature at the crimping point of the wire core is the highest, reaching 81.2 °C. As the

temperature measurement point moves away from the cable joint, the temperature of the cable core gradually decreases and eventually approaches 44 °C.

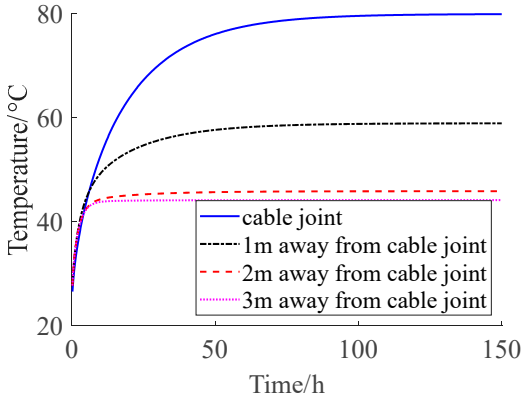


Figure 3. Temperature curve at different positions of cable core.

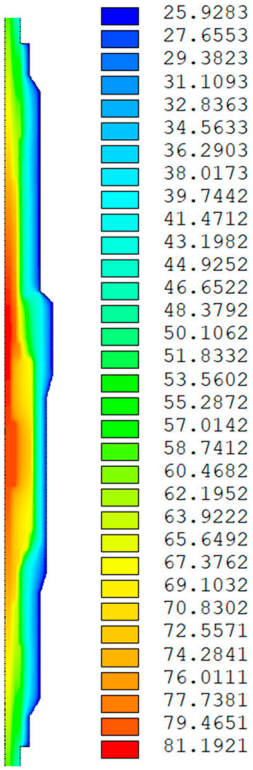


Figure 4. Steady temperature distribution of cable joint.

2.2. Analysis of the Temperature Field Calculation Results

From the temperature field calculation results, it can be seen that the internal core temperature of the joint is relatively high, and the temperature rapidly decreases along the radial direction. At the same time, the temperature gradually decreases when extending upwards towards both sides of the main body. This is because there is contact resistance in the intermediate joint, and its heat generation rate is relatively high. And due to the presence of a waterproof adhesive layer with low thermal conductivity and high thermal resistance at the joint, the radial heat dissipation capacity of the intermediate joint is weaker than that of the cable body, resulting in a higher temperature at the intermediate joint. Therefore, although the middle joint mainly dissipates heat radially, a portion of the heat is also transferred axially, and there are two heat dissipation paths in the cable joint, radial and axial. By separately extracting the steady-state temperature change curves

of the radial and axial directions at the crimping point, the obtained results are shown in Figure 5. It can be seen that due to the different material properties of each layer, the radial temperature gradient of cable joints varies greatly. According to the radial temperature distribution, the radial heat dissipation path of the intermediate joint mainly includes conductors, rubber prefabricated parts, waterproof glue, and three materials. The smaller the thermal conductivity of the materials, the greater the corresponding thermal resistance, and the larger the temperature gradient in this area in the steady-state results. At the same time, there will be a small horizontal area in the radial temperature distribution of the waterproof adhesive position, corresponding to thin-walled structures with high thermal conductivity such as copper shells and fiberglass shells.

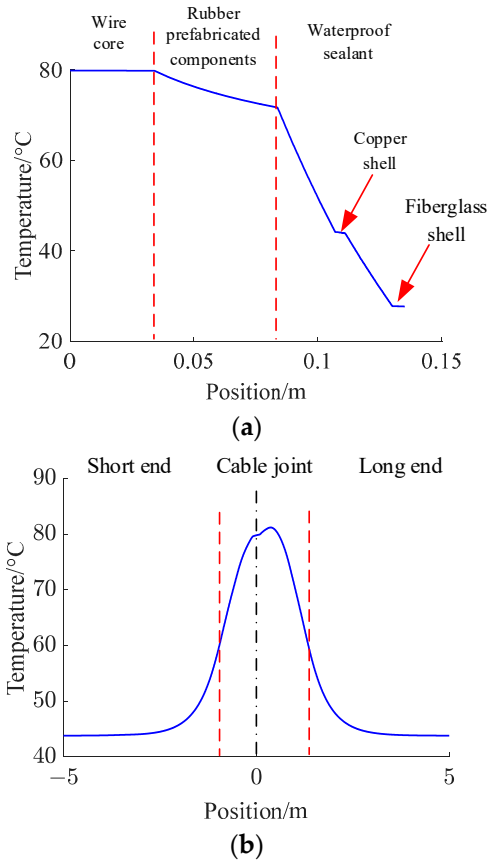


Figure 5. Radial and axial steady-state temperature distribution at cable joint. (**a**) Radial temperature distribution. (**b**) Axial temperature distribution.

Comparing the radial temperature distribution at the pressure connection point and the joint end, it can be found that although the core temperature at the joint end is lower, due to the small radial thermal resistance at the joint end, the cable core has good heat dissipation effect, and the skin temperature is actually higher than that at the pressure connection point.

The axial temperature of the wire core can be seen from the temperature distribution curve. The temperature of the cable core inside the joint is relatively high, and the temperature gradually decreases when extending towards both sides of the main body. After being 4 m away from the center, the temperature tends to balance, showing an overall convex curve. For the joint section, it can be seen that the temperature at the crimping point is relatively high, about 80 °C. But the distribution is relatively uniform, and the temperature rapidly decreases near the joint end. The temperature at the joint end corresponding to the long and short ends is about 60 °C.

In summary, the middle joint of the cable not only has radial heat dissipation, but also axial heat dissipation. When establishing a thermal path model, two directions of

heat dissipation paths need to be considered. Based on the changes in radial and axial temperature distribution, a simplified thermal circuit model can be established.

3. Equivalence Analysis of Thermal Circuit Models

3.1. Cable Joint Thermal Circuit Model

Due to the radial and axial heat dissipation paths of the cable joint core, the core of the main body will also dissipate heat along the radial direction. Therefore, the thermal diffusion of the cable body and intermediate joints can be described using a segmented thermal resistance network, as shown in Figure 6. Among them, ΔP_j is the heat flux generated by the conductor element at the cable joint, and ΔP_c is the heat flux generated by the conductor element in the body. Considering the high temperature and low thermal resistance of the wire core, the heat flow is mainly transmitted along the wire core in the axial direction. Therefore, the axial heat transfer of the outer structures of the wire core is ignored in the thermal resistance network. Axial heat dissipation is divided into several microelements, which are connected by the thermal resistance of conductors. Radial heat dissipation includes radial heat dissipation of the joint and radial heat dissipation of the body. According to the structure of the cable, the radial heat dissipation of the joint includes multi-layer thermal resistance such as rubber prefabricated parts, waterproof glue, copper shells, fiberglass shells, and air. The radial heat dissipation of the body includes a cross-linked polyethylene insulation layer (XLPE), water barrier tape, aluminum sheath, outer sheath, air, and multiple layers of thermal resistance.

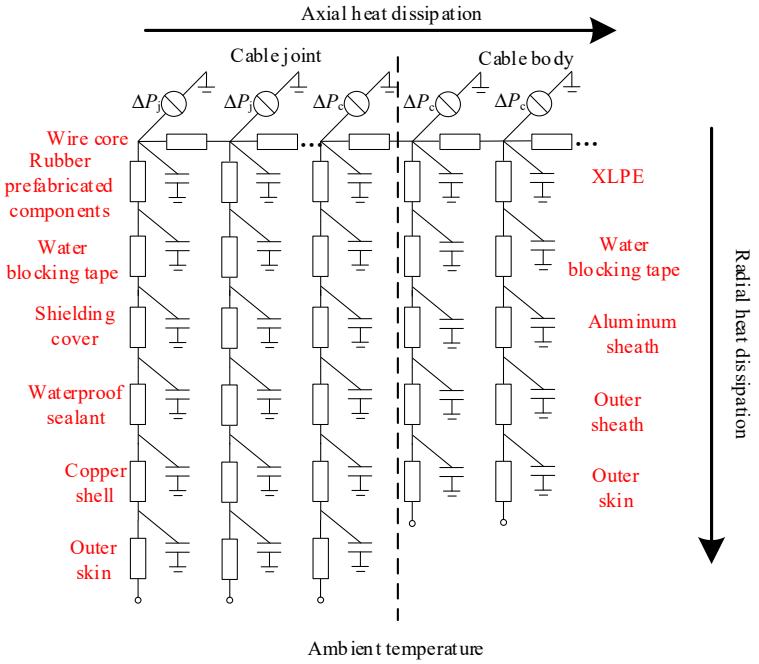


Figure 6. Thermal resistance network model of cable joint.

Considering computational efficiency, it is necessary to simplify the thermal resistance network model and transform the axial microelement model into a suitable centralized parameter model for calculation while ignoring some components with lower thermal resistance. The joint part is simplified as a one-dimensional thermal circuit model. Considering the small thickness and low thermal resistance of the copper shell and fiberglass shell, the waterproof adhesive, copper shell, waterproof adhesive and fiberglass shell layer outside the original rubber prefabricated component is simplified into a single layer of waterproof adhesive, and the entire radial heat dissipation is simplified into a three-layer thermal resistance of rubber prefabricated components, waterproof adhesive and air. Due to the main focus on the hotspot temperature of the joint, for the body part, it is simplified as a

form of thermal resistance plus a temperature rise of the cable body core. In summary, the simplified thermal circuit model is shown in Figure 7.

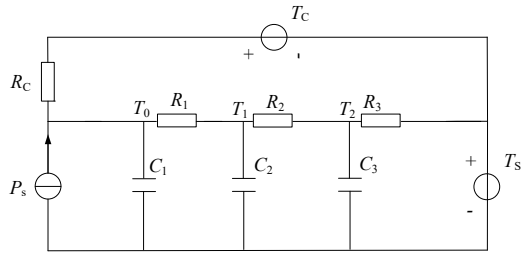


Figure 7. Simplified thermal circuit model of cable joint.

Where P_s is the heating power of the neutral core in the joint; C_1~C_3 and R_1~R_3, respectively, represent the equivalent heat capacity and thermal resistance of the three-layer materials, i.e., rubber prefabricated parts, waterproof rubber, and air; T_s is the ambient temperature; R_c is the equivalent thermal resistance for axial heat dissipation of cable joints; and T_c is the transient temperature rise of the cable body core. According to the structure of the cable body, calculations can be made using a transient thermal circuit model. T_0 is the hotspot temperature of the wire core, T_1 is the outer surface temperature of the rubber prefabricated component, and T_2 is the skin temperature of the cable joint.

3.2. Transient Thermal Path Model Solution

By writing the state equation of a simplified thermal circuit model, transient processes can be solved [29,30]. According to KCL, the following circuit equations can be written for the thermal circuit model.

$$\begin{cases} C_1\frac{dT_0}{dt}+\frac{T_0-T_1}{R_1}+\frac{T_0-T_c-T_s}{R_c}-P_s=0 \\ \frac{T_0-T_1}{R_1}+\frac{T_2-T_1}{R_2}-C_2\frac{dT_1}{dt}=0 \\ \frac{T_1-T_2}{R_2}+\frac{T_s-T_2}{R_3}-C_3\frac{dT_2}{dt}=0 \end{cases} \tag{3}$$

By organizing the above equations, the state equation of the transient thermal circuit model can be obtained:

$$\begin{bmatrix} \frac{dT_0}{dt} \\ \frac{dT_1}{dt} \\ \frac{dT_2}{dt} \end{bmatrix} = \begin{bmatrix} \frac{-(R_1+R_c)}{R_1R_cC_1} & \frac{1}{R_1C_1} & 0 \\ \frac{1}{R_1C_2} & \frac{-(R_1+R_2)}{R_1R_2C_2} & \frac{1}{R_2C_2} \\ 0 & \frac{1}{R_2C_3} & \frac{-(R_2+R_3)}{R_2R_3C_3} \end{bmatrix} \begin{bmatrix} T_0 \\ T_1 \\ T_2 \end{bmatrix} + \begin{bmatrix} \frac{1}{C_1} & \frac{1}{C_1R_c} & \frac{1}{C_1R_c} \\ 0 & 0 & 0 \\ 0 & \frac{1}{R_3C_3} & 0 \end{bmatrix} \begin{bmatrix} P_s \\ T_s \\ T_c \end{bmatrix} \tag{4}$$

The above equation can be written as the general form of the state equation:

$$\dot{\boldsymbol{T}} = \boldsymbol{AT} + \boldsymbol{BU} \tag{5}$$

where $\boldsymbol{T}(t)$ is the three-dimensional state vector, $\boldsymbol{T}(t) = [T_0(t), T_1(t), T_2(t)]^T$. This corresponds to the temperature of each node in the thermal path model. $\dot{T}$ is the derivative of $\boldsymbol{T}(t)$ over time. A and B are both real-constant-coefficient matrices. U is the input column vector, where $\boldsymbol{U} = [P_s(t), T_s(t), T_c(t)]^T$. By approximating the derivative $\dot{T}$ in Equation (5) as a difference, we can obtain the following:

$$\frac{\boldsymbol{T}(t+\Delta t)-\boldsymbol{T}(t)}{\Delta t} = \boldsymbol{AT}(t+\Delta t)+\boldsymbol{BU} \tag{6}$$

In the formula, E is the identity matrix. By selecting a reasonable time step, the temperature of each node during the transient process can be calculated according to the above equation. In summary, the process of calculating the temperature rise of the wire core through the transient thermal circuit model is shown in Figure 8. Firstly, the core temperature rise $T_c(t)$ of the cable body at time t can be solved through the thermal circuit model of the cable body, and then it can be used as an input to the state equation of the transient thermal circuit model of the cable joint. By approximating the difference, the temperature $\boldsymbol{T}(t + \Delta t)$ of each node at the next moment is solved, and the temperature change in the transient process is obtained through continuous iteration. Due to its ability to obtain analytical solutions through matrix operations, this method has a faster computational speed compared to finite element field calculations.

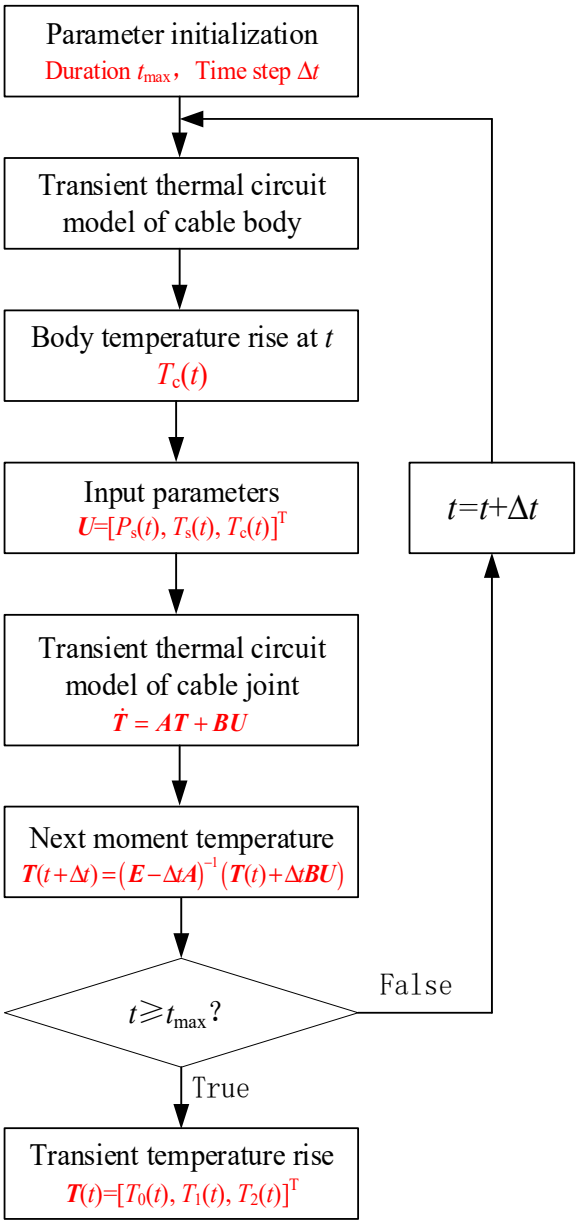


Figure 8. Calculation process of transient temperature rise of cable joint.

4. Verification of Joint Temperature Inversion Model

4.1. Transient Temperature Rise Calculation of Cable Body

Due to the fact that the temperature rise of the remote cable body is only related to the cross-sectional structure of the cable and not to the cable joint, the transient temperature rise of the cable core can be independently calculated first, and then incorporated into the model of the cable joint for calculation. For the five-layer structure of the XLPE–water blocking tape–aluminum sheath–outer sheath–air of the cable body, considering the small thickness and high thermal conductivity of the aluminum sheath layer, the thermal resistance of this layer structure is low and the temperature change is small, so this layer structure is ignored when establishing the thermal circuit model. The thermal conductivity, density, specific heat, and other parameters of the water barrier are similar to those of the outer sheath, and the thickness of this layer structure is also very small. Therefore, when simplifying the thermal circuit model, this layer is merged with the outer sheath layer. The heat dissipation path of the final cable body is simplified as the three-layer XLPE–outer sheath–air, as shown in Figure 9. Among them, P_c is the heating power of the cable body core; C_{1c}~C_{3c} and R_{1c}~R_{3c} represent the equivalent heat capacity and thermal resistance of XLPE, outer sheath, and air layers, respectively; T_c is the temperature of the cable body core; T_{1c} is the outer surface temperature of the XLPE layer; and T_{2c} is the skin temperature of the cable body.

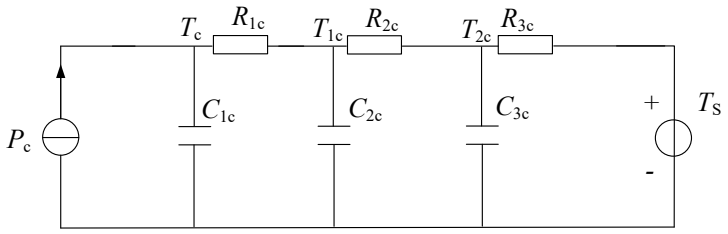


Figure 9. Simplified thermal circuit model of cable body.

The transient temperature changes of each layer are calculated using a thermal path model, and compared with the calculation results of the temperature of each layer of the remote cable body in finite element simulation, as shown in Figure 10. It can be seen that the temperature changes of the cable body calculated by the simplified thermal path model are consistent with the finite element calculation results, verifying the effectiveness of the cable body thermal path model. After about 20 h, the temperature of each layer of the cable body reached a steady state, and the steady-state temperatures of the wire core, XLPE layer, and body skin were 43.8 °C, 35.8 °C, and 33.0 °C, respectively.

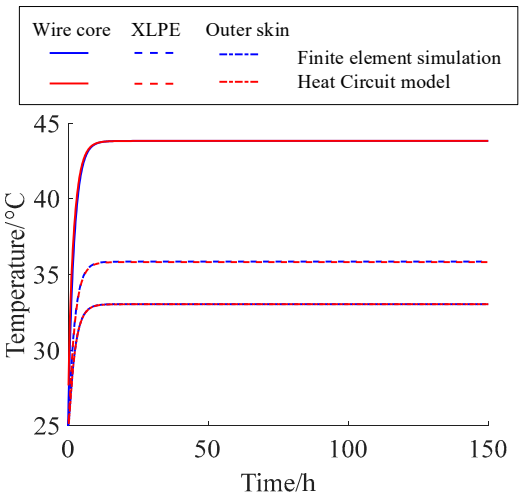


Figure 10. Calculation results of cable body thermal circuit model.

4.2. Transient Temperature Rise Calculation of Cable Joints

On the basis of calculating the transient temperature changes of the cable body, the transient temperature rise of the body core can be extracted. By introducing the state equation of Equation (4), the temperature changes of cable joints during transient processes can be further calculated. The temperature changes of the cable joint core, rubber prefabricated outer layer, and cable joint outer skin can be calculated and compared with the results of finite element simulation, as shown in Figure 11. It can be seen that the transient temperature changes of each layer of the cable joint calculated by simplifying the thermal circuit model are consistent with the results of finite element simulation. To further verify the calculation error of the simplified model, the maximum values of steady-state temperature calculation error and transient process temperature calculation error for each layer are extracted, as shown in Table 2. It can be seen that compared with the finite element calculation results, the steady-state temperature error calculated by the thermal circuit model does not exceed 1 °C, and the maximum temperature error of the transient process does not exceed 3 °C. This indicates that the proposed thermal path model has good consistency with the finite element calculation results, verifying the effectiveness of the thermal path model. In addition, using the thermal path model results in a faster calculation speed and better engineering application prospects.

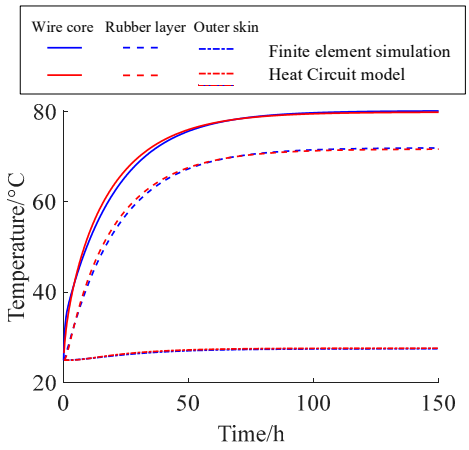


Figure 11. Calculation results of cable joint thermal circuit model.

Table 2. Calculation error of cable joint thermal circuit model.

Location of Temperature Extraction	Steady-State Temperature Error	Transient Maximum Temperature Error
Joint core	0.28	2.88
Outer layer of rubber prefabricated components	0.27	1.38
Joint outer skin	0.13	0.21

The calculation of the cable's current-carrying capacity is usually based on the inversion of core temperature, so it is often necessary to collect skin temperature to perceive core temperature. Comparing the calculation results of the cable body and cable joints, it can be seen that the temperature rise of the joint core is much higher than that of the cable body. However, due to the large thickness of the joint and the low thermal conductivity of the filling material, the temperature rise of the joint skin is actually lower than that of the cable body. The temperature of the wire core inside the cable joint can be inferred from the surface temperature of the cable joint, which may result in significant errors. Due to the axial heat dissipation of cable joints, the temperature rises of the cable body skin adjacent to the joint will also be affected by the temperature rise of the joint core. Therefore, in

practical engineering applications, the sensing of the joint core temperature can be achieved by collecting the skin temperature of the cable body near the joint.

The proposed method in this paper gives a new approach to quickly calculate the temperature of cable core hotspots while balancing computational efficiency. Although the finite element method can calculate more accurate results, it requires continuous iteration to calculate the finite element model. Therefore, calculating transient temperature requires a considerable amount of time, which is not conducive to the real-time acquisition of cable core temperature in engineering. On the other hand, after cable installation is completed, the structure of the cable can be considered unchanged, so the temperature of cable core hotspots is mainly determined by the transient current. Under real-time monitoring of the current, the real-time temperature can be calculated rapidly according to the thermal circuit model proposed in this paper, providing reference for the status monitoring of cable joints.

5. Conclusions

This article establishes a simplified thermal circuit model for cable joints considering axial heat dissipation, and takes 110 kV cable joints as an example to calculate transient temperature rise. Compared with finite element calculation methods, the following conclusions are obtained:

(1) The radial thermal resistance of the intermediate joint is greater than that of the cable body, and the core temperature of the joint is greater than that of the body core, which will generate axial heat dissipation. When establishing a thermal path model, axial heat dissipation needs to be considered.

(2) The axial heat dissipation of cable joints can be equivalent to thermal resistance plus the temperature rise of the cable core, and an equivalent thermal circuit model of cable joints can be established. Compared with the finite element calculation results, the steady-state temperature error of the thermal circuit model does not exceed 1 °C, and the maximum temperature error of the transient process does not exceed 3 °C.

(3) The temperature of the cable joint skin is lower than that of the cable body skin. In engineering applications, the temperature of the joint core can be sensed by the temperature of the adjacent cable body skin, which improves sensitivity.

Author Contributions: Conceptualization, Z.Z. and Y.C.; methodology, X.D.; software, L.L.; validation, X.W. and J.R.; writing—original draft preparation, Z.Z., X.D., L.L., X.W., Y.C. and J.R. All authors have read and agreed to the published version of the manuscript.

Funding: This research was funded by National Natural Science Foundation of China (No. U2066217) and the Science and Technology Program of China Southern Power Grid (No. GDKJXM20220135).

Data Availability Statement: Data are contained within the article.

Conflicts of Interest: Authors Zhiqiang Zhang, Xiaolong Deng, Lili Liang, Yu Chen were employed by the company China Southern Power Grid Co., Ltd. The remaining authors declare that the research was conducted in the absence of any commercial or financial relationships that could be construed as a potential conflict of interest.

References

1. Zhou, Y.X.; Zhao, J.K.; Liu, R.; Chen, Z.Z.; Zhang, Y.X. Key technical analysis and prospect of high voltage and extra-high voltage power cable. *High Volt. Eng.* **2014**, *40*, 2593–2612.
2. Guo, W.; Zhou, S.L.; Wang, L.; Pei, H.; Zhang, C.; Li, H.C. Design and application of online monitoring system for electrical cable states. *High Volt. Eng.* **2019**, *45*, 3459–3466.
3. Peng, C.; Zhang, Y.J.; Qin, W.N. Study on insulation performance of EHV power cable joint based on finite volume method. *High Volt. Eng.* **2014**, *40*, 3695–3701.
4. Zhu, X. Research on Key Status Monitoring and Evaluation Technology of Distribution Equipment. Ph.D. Thesis, North China Electric Power University, Beijing, China, 2017.
5. Zhou, L.; Cao, J.; Wang, S.; Liu, L.; Yang, Y.; Jiang, H. Comprehensive state evaluation of high voltage cable based on multi-state variables characteristics and variation law. *High Volt. Eng.* **2019**, *45*, 3954–3963.
6. Liang, Y. Technological development in evaluating the temperature and ampacity of power cables. *High Volt. Eng.* **2016**, *42*, 1142–1150.

7. Li, H.; Li, J.; Ma, Y.; Yan, Q.M. Effects of thermal aging on the crystal structures of the XLPE cable insulating material at different temperatures. *Proc. CSEE* **2017**, *37*, 6740–6748.
8. Jiayin, B.; Yonglan, L.; Luping, S. Analysis of steady-state heat path model and calculation of current carrying capacity for 500 kV power cable. *Insul. Mater.* **2019**, *52*, 96–101.
9. Liulin, Y.; Zhenlin, X. Cable joint temperature monitoring system based on narrow-band internet of things. *Sci. Technol. Eng.* **2022**, *22*, 2275–2283.
10. *IEC Publication 60287*; Calculation of the Continuous Current Ratings of Cables. IEC: Geneva, Switzerland, 1982.
11. *IEC Standard 60853-1*; Calculation of the Cyclic and Emergency Current Ratings of Cables. Part I: Cyclic Rating Factor for Cables up to and Including 18/30 (36) kV. Publication 853-1. IEC: Geneva, Switzerland, 1985.
12. *IEC Standard 60853-2*; Calculation of the Cyclic and Emergency Current Ratings of Cables. Part 2: Cyclic Rating Factor of Cables Greater than 18/30 (36) kV and Emergency Ratings for Cables of All Voltages. Publication 853-2. IEC: Geneva, Switzerland, 1989.
13. Gela, G.; Dai, J.J. Calculation of thermal fields of underground cables using the boundary element method. *IEEE Trans. Power Deliv.* **1988**, *3*, 1341–1347. [CrossRef]
14. Olsen, R.; Anders, G.J.; Holboell, J. Modeling of dynamic transmission cable temperature considering soil-specific heat, thermal resistivity, and precipitation. *IEEE Trans. Power Deliv.* **2013**, *28*, 1909–1917. [CrossRef]
15. Zhan, Q.; Xiao, W.; Luo, R.; Tan, T. The temperature monitoring of cable joint conductor based on transient thermal circuit model and inversion algorithm. *South. Power Syst. Technol.* **2014**, *8*, 83–87.
16. Gao, Y.; Tan, T.; Liu, K.; Ruan, J. Research on temperature retrieval and fault diagnosis of cable joint. *High Volt. Eng.* **2016**, *42*, 535–542.
17. Wang, Z. Theoretical Analysis and Experimental Research on Current Carrying Hotspots in 110 kV Cable Lines. Ph.D. Thesis, South China University of Technology, Guangzhou, China, 2017.
18. Tong, Z.J.; Zhou, N.R.; Duan, Q.S.; He, C.; Wang, Y.C.; Jin, X.T. Research on temperature detection of T type cable joint conductor of ring network cabinet based on thermal circuit method. *Transducer Microsyst. Technol.* **2017**, *36*, 131–134+138.
19. Bragatto, T.; Cresta, M.; Gatta, F.M.; Geri, A.; Maccioni, M.; Paulucci, M. A 3-D nonlinear thermal circuit model of underground MV power cables and their joints. *Electr. Power Syst. Res.* **2019**, *173*, 112–121. [CrossRef]
20. Liu, G.; Lei, M.; Ruan, B.; Zhou, F.; Li, Y.; Liu, Y. Model research of real-time calculation for single-core cable temperature considering axial heat transfer. *High Volt. Eng.* **2012**, *38*, 1877–1883.
21. Lin, D.; Zhang, X.Y.; Wang, P.Y.; Liu, L.F.; Mao, J.K.; Xu, T. Experimental study of the axial heat transfer for HV cable joint. *Electr. Wire Cable* **2017**, 5–10. [CrossRef]
22. Ruan, J.; Zhang, Y.; Wang, D.; Shu, S.; Qiu, Z. Numerical simulation research and applications of electromagnetic multiphysical field for electrical equipment. *High Volt. Eng.* **2020**, *46*, 739–756.
23. Ilie, S.; Toader, D.; Barvinschi, F. Modern education on renewable energies by using numerical Finite Element Method of a solar powered Stirling engine with heat transfer simulations. In Proceeding of the 2016 12th IEEE International Symposium on Electronics and Telecommunications (ISETC), Timisoara, Romania, 27–28 October 2016.
24. Arvinti, B.; Toader, D.; Vesa, D.; Costache, M. Experimental and Analytical Study of the Electric Potential using Lagrange Polynomials. In Proceeding of the 2020 International Symposium on Electronics and Telecommunications (ISETC), Timisoara, Romania, 5–6 November 2020.
25. Zhao, X.F.; Hao, Y.F.; Huang, G.Q. Calculation on steady-state current carrying capacity of intermediate joint of direct buried cable based on the finite element simulation. *High Volt. Appar.* **2022**, *58*, 64–70+85.
26. Liu, H.C.; Zhang, M.J.; Liu, Y.P.; Zhang, A.J.; Xu, X.B. Experimental and simulation study of dynamic ampacity characteristics for ±160 kV XLPE DC submarine cable. *Electr. Meas. Instrum.* **2020**, *57*, 19–27.
27. Lei, C.; Liu, G.; Li, Q. Dynamic calculation of conductor temperature of single-cable using BP neural network. *High Volt. Eng.* **2011**, *37*, 184–189.
28. Liu, C.; Ruan, J.J.; Huang, D.C.; Zhan, Q.H.; Xiao, W. Hot spot temperature of cable joint considering contact resistance. *High Volt. Eng.* **2016**, *42*, 3634–3640.
29. Ying, Z.; Du, Z.; Feng, K.; Liu, Y.; Wu, J. Radial thermal circuit model and parameter calculation method for high voltage overhead transmission line. *Trans. China Electrotech. Soc.* **2016**, *31*, 13–21.
30. Ying, Z.; Kai, F.; Du, Z.; Liu, Y.; Wu, J. Thermal circuit modeling of the relationship between current and axial temperature for high voltage overhead conductor. *Proc. CSEE* **2015**, *35*, 2887–2895.

Disclaimer/Publisher's Note: The statements, opinions and data contained in all publications are solely those of the individual author(s) and contributor(s) and not of MDPI and/or the editor(s). MDPI and/or the editor(s) disclaim responsibility for any injury to people or property resulting from any ideas, methods, instructions or products referred to in the content.